

FLAP: Fully-controllable Audio-driven Portrait Video Generation through 3D head conditioned diffusion model

Lingzhou Mu¹ Baiji Liu² Ruonan Zhang¹ Guiming Mo² Jiawei Jin¹ Kai Zhang¹ Haozhi Huang²

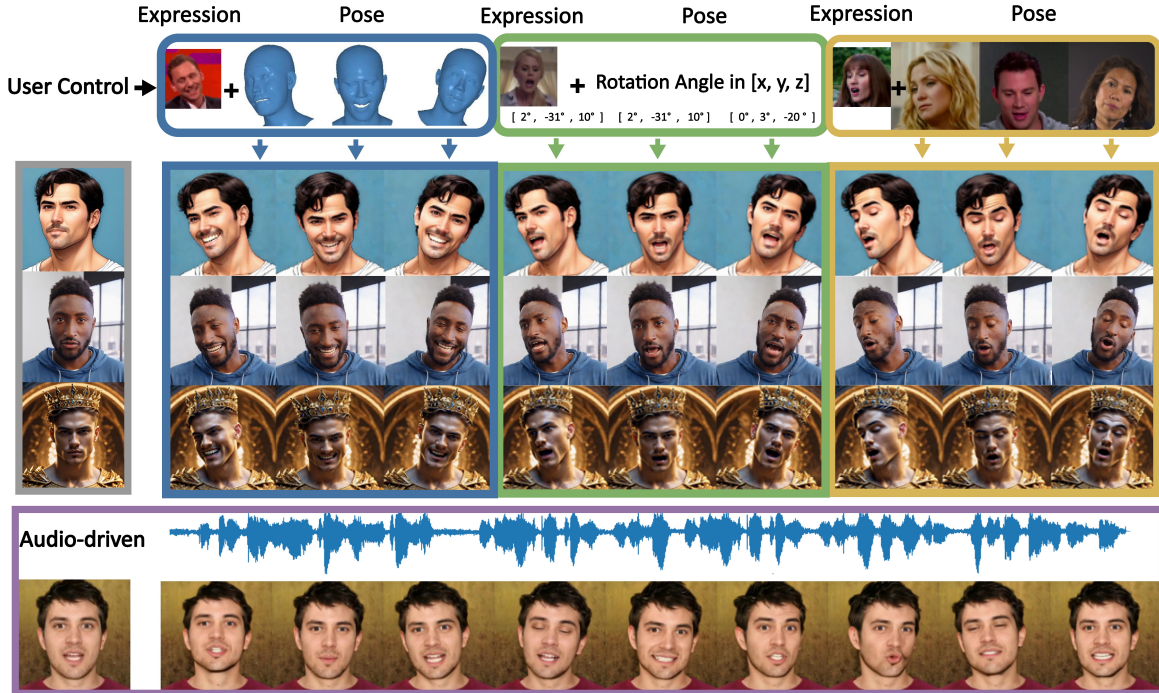


Figure 1. FLAP offers full controllability by supporting various types of control signals

Abstract

Diffusion-based video generation techniques have significantly improved zero-shot talking-head avatar generation, enhancing the naturalness of both head motion and facial expressions. However, existing methods suffer from poor controllability, making them less applicable to real-world scenarios such as filmmaking and live streaming for e-commerce. To address this limitation, we propose FLAP, a novel approach that integrates explicit 3D intermediate parameters (head poses and facial expressions) into the diffusion model for end-to-end generation of realistic portrait videos. The proposed architecture allows the model to generate vivid portrait videos from audio while simultaneously incorporating additional control signals, such as head rotation an-

gles and eye-blinking frequency. Furthermore, the decoupling of head pose and facial expression allows for independent control of each, offering precise manipulation of both the avatar’s pose and facial expressions. We also demonstrate its flexibility in integrating with existing 3D head generation methods, bridging the gap between 3D model-based approaches and end-to-end diffusion techniques. Extensive experiments show that our method outperforms recent audio-driven portrait video models in both naturalness and controllability.

1. Introduction

Portrait video generation, or zero-shot talking-head avatars, aims to animate a static portrait image using speech audio or video. Diffusion-based methods have demonstrated high precision in lip synchronization, realistic facial behavior,

and natural head movements through specialized modules and network architectures.

However, in practical applications like live streaming for e-commerce or film production, naturalness alone is insufficient. For example, in filmmaking, an avatar should turn its head toward someone before starting a conversation. Additionally, avatars are often required to perform specific motions, such as nodding or head-shaking, as dictated by the film script.

As alternatives, LivePortrait (Guo et al., 2024) and MegActor (Yang et al., 2024) use video as input to generate head motions and expressions based on reference videos. These methods transform the challenge into an expression mapping task. However, by requiring additional video input to specify target expressions and motions, their usability is limited. Earlier GAN-based methods (Burkov et al., 2020; Zhou et al., 2021) separate faces into identity and non-identity components, leveraging identity consistency and pose variation across frames. However, these methods still produce unnatural videos, with restricted pose variations and severe identity loss, resulting in faces that often appear generic. The closest attempt, VASA-1 (Xu et al., 2024b), uses FaceVid2Vid (Wang et al., 2021) and Mega-Portrait (Drobyshev et al., 2022) as its motion-to-video model, while generating the motion input via a diffusion model. Although this approach enhances Mega-Portrait’s control by synthesizing controllable motion inputs, it still relies on the original Mega-Portrait for head rotation control, leading to the same generic face issue.

In contrast, more recent works use diffusion-based models to achieve superior naturalness, but at the cost of reduced controllability. For example, EchoMimic (Chen et al., 2024), Ani-portrait (Wei et al., 2024) and Follow-Your-Emoji (Ma et al., 2024b) introduce 2D motion fields based on selected landmarks. These landmark based approaches project facial landmarks into 2D image and combines them with noisy latent variables to guide the diffusion process, resulting in three major drawbacks. 1) Projecting landmarks into 2D image space destroys the 3D information, hindering the model’s ability to learn 3D structure. 2) Simply adding 2D landmark images to noisy latents destroys the translation invariance, requiring additional alignment (Ma et al., 2024b; Wang et al., 2024a) between the input landmarks and the reference face. 3) Facial landmarks are suboptimal as control signals for human faces, as they provide vague semantic information and are entangled with identity. Using this vague and entangled information as a primary control signal significantly limits the potential of diffusion models. Furthermore, most end-to-end diffusion-based models (Xu et al., 2024a; Tian et al., 2024; Jiang et al., 2024; Cui et al., 2024) do not support user-specified control signals, ignoring the importance of controllability.

To address this limitation and enhance model usability across various scenarios, we present a novel approach called FLAP. As shown in Figure 1, FLAP can generate natural head movements from audio or replace these movements with user-defined actions, such as turning, tilting, looking around, or even jerking. FLAP supports six degrees of freedom (6DoF) for control over head movements, demonstrating its nuanced understanding of 3D space. In addition to motion control, FLAP can generate lifelike expressions from three sources: audio, user-specified expression coefficients, and coefficients extracted from images or videos. Each of these sources can be used independently or combined to create new expressions. For example, as shown in when no control signal is provided, FLAP generates a talking-head video with natural expressions and mild head movements from audio alone. When expressions are provided by an image with a user-modified head pose, FLAP generates the corresponding talking-head video.

In summary, our contributions are as follows: 1) We introduce FLAP, a diffusion-based framework that produces high controllability while maintaining naturalness and high precision in lip synchronization. 2) To the best of our knowledge, FLAP is the very first work that utilizes 3D head coefficients as diffusion conditions. This not only enhanced its controllability, but also brings flexibility in integrating with existing 3D head generation methods, bridging the gap between 3D model-based approaches and end-to-end diffusion techniques. 3) We propose a Progressively Focused Training scheme for expression-motion decoupling, in which facial expression conditions and head pose are progressively focused and learned. This ensures independent control of facial expression and head motion.

2. Related Works

2.1. Non-diffusion-based Portrait Animation

For non-diffusion-based models, previous approaches (Zhou et al., 2020; Chen et al., 2019) mainly introduce intermediate representation and leverage Generative Adversarial Networks (GANs) (Goodfellow et al., 2020) to generate final images. These methods first train an audio-to-motion model to predict head motion from audio, and then warp head motion into video. For example, AudioDVP (Wen et al., 2020) use BFM (Paysan et al., 2009) parameters as intermediate representation for motion, predicting mouth related parameters for reenactment. FaceVid2vid (Wang et al., 2021) introduced 3D implicit keypoints to further enhance the representation efficiency for warping and reenactment. CodeTalker (Xing et al., 2023) replace BFM with FLAME (Li et al., 2017) improving expressiveness of keypoints. As for audio-to-motion models, recent works (Fan et al., 2022; Gong et al., 2023) introduced transformer based models to enhance long sequences generalization ability and cross-

modal alignment. GeneFace (Ye et al., 2023) proposed a variational motion generator to predict landmark sequence from audio and designed a 3DMM nerf render to solve mean face problem. More recent works like Liveportrait (Guo et al., 2024) introduced a mixed image-video training strategy, with a upgraded network architecture and a much larger training dataset. It achieved effectively balance of the generalization ability, computational efficiency, and controllability, yet requires video input as motion source.

2.2. Diffusion-based Portrait Animation

Diffusion models (DMs) (Ho et al., 2020; Song et al., 2020) achieves superior performance in various generative tasks including image generation (Rombach et al., 2022; Ruiz et al., 2023; Shi et al., 2024) and editing (Brooks et al., 2023; Cao et al., 2023), video generation (He et al., 2022; Ma et al., 2024a; Wang et al., 2024b) and editing (Li et al., 2024; Qi et al., 2023; Zhang et al., 2023c). Extensive studies (Zhang et al., 2023a; Li et al., 2025; Hu et al., 2021; Rombach et al., 2022) have proven the feasibility of controlling image generation process with condition signal such as text, landmarks, segmentations, dense poses and encoded images.

Relevant to our task of portrait animation, most recent approaches (Tian et al., 2024; Chen et al., 2024; Wang et al., 2024a; Xu et al., 2024a; Ma et al., 2024b) employed a dual U-Net architecture similar to AnimateAnyone (Hu, 2024) and incorporate temporal module (Guo et al., 2023) into generation process. Besides, EMO (Tian et al., 2024) also employed face location mask and head speed as control signals using controlnet-based mechanism and attention-based mechanism respectively. Following such a paradigm, EchoMimic (Chen et al., 2024), V-Express (Wang et al., 2024a) and Follow-your-emoji (Ma et al., 2024b) integrate facial landmark conditions by adopting ControlNet (Zhang et al., 2023a) mechanism. X-portrait (Xie et al., 2024) proposed a ControlNet-based motion control module with local masking and scaling mechanism to achieve fine-grained motion control. Hallo2 (Cui et al., 2024) and Instruct Avatar (Wang et al., 2024c) integrate text condition as a guidance for diffusion process. VASA-1 proposed a motion space DiT (Peebles & Xie, 2023) with eye gaze direction, head-to-camera distance and emotion offset as condition to generate motion latent. For motion-to-video module, it relied on a retrained FaceVid2Vid (Wang et al., 2021) and MegaPortrait (Drobyshev et al., 2022) to render final video result.

Apart from studies on control signals, another branch of existing studies focus on enhancing the alignment between audio, expression and head motion. For example, Hallo (Xu et al., 2024a) proposed a hierarchical audio-driven visual synthesis module to enhance audio-visual correlation. Loopy (Jiang et al., 2024) transformed audio feature and landmark feature into a same latent space to ensure strong

dependency between audio and head motion.

2.3. Disentanglement on Talking Head Representation

Disentangled controlling of lip pose, expressions, and head movement is a longstanding task in talking head generation. The main target of this task is to decouple these features of a portrait video, so we can achieve independent manipulation of each. (Siarohin et al., 2019) utilize explicit 2D keypoints to characterize facial dynamics. But these 2D keypoints carry insufficient head pose information in 3D space and carry identity information. Other explicit approaches like 3D face models such as BFM (Paysan et al., 2009) and FLAME (Li et al., 2017) can fit head pose and expression accurately while remaining editable, but they suffer from issues such as identity loss or lack of effective rendering methods. As solutions for expressiveness, implicit approaches such as PC-AVS (Zhou et al., 2021) employs contrastive learning to isolate the mouth space related to audio. PD-FGC (Wang et al., 2023) extended PC-AVS by progressively disentangle identity, head pose, eye gaze direction and emotion after lip pose isolated by PC-AVS. Following this line, EDTalk (Tan et al., 2025) introduce a lightweight framework with orthogonal bases, and reduced training cost without performance degradation. However, the introduce of implicit features requires a preset discrete style label (Wang et al., 2023; Tan et al., 2025) or additional video as input, which reduces style diversity or cause inconvenience.

3. Preliminaries

3.1. Latent Diffusion Model

Latent diffusion models (LDM) (Rombach et al., 2022) are a class of diffusion models that operate diffusion process in latent space, achieving stable and fast generation. At each diffusion time step t , the noisy latent z_t is fed into the network and performs cross-attention with condition c . Then network predicts ϵ conditioned on the given text or other prompts c . The overall training objective can be formulated as follows:

$$L_{LDM} = \mathbb{E}_{z_t, c, \epsilon \sim \mathcal{N}(0,1), t} [\|\epsilon - \epsilon_\theta(z_t, t, C)\|_2^2] \quad (1)$$

where ϵ_θ denotes denoising net. In Stable Diffusion (SD), C represents text prompts c_{text} , image prompts c_{img} or both $C = [c_{text}, c_{img}]$. In the field of portrait animation, condition C includes reference image, audio, context frames, landmarks and other additional information.

3.2. 3D Morphable Face Model

The research in 3D morphable face modeling aims to accurately capture, parameterize, and reconstruct human face using statistical models. As a fundamental 3D morphable face model, FLAME (Li et al., 2017) is widely adopted in

numerous research works (Daněček et al., 2022; 2023; Qian et al., 2024). FLAME use standard vertex based linear blend skinning (LBS) with blendshapes, with $N_v = 5023$ vertices, $k = 4$ joints (neck, jaw, and eyeballs), and $N_f = 9976$ facets. Formally, FLAME is described by a function

$$M(\beta, \theta, \psi) \rightarrow (\mathbf{V}, \mathbf{F}), \quad (2)$$

which parameterize 3D human face into identity shape $\beta \in \mathbb{R}^{|\beta|}$, facial expression $\psi \in \mathbb{R}^{|\psi|}$, and pose parameters $\theta \in \mathbb{R}^{3k+3}$ for rotations around $k = 4$ joints (neck, jaw, and eyeballs) and global rotations. Each rotation vector of pose parameters is represented by axis angles ($\in \mathbb{R}^3$). Given these parameters, FLAME outputs a 3D mesh with vertices $\mathbf{V} \in \mathbb{R}^{N_v \times 3}$ and facets $\mathbf{F} \in \mathbb{R}^{N_f \times 3}$.

4. Methodology

4.1. Overall Framework

FLAP is build upon Stable Diffusion (SD) and AnimateDiff (Guo et al., 2023) utilizing their weights for initialization. Following recent diffusion-based portrait animation methods (Hu, 2024), we employed a dual U-net architecture which consists of two U-Nets initialized with SD 1.5. In this architecture, one of the U-nets, namely ReferenceNet, works as reference image encoder and, therefore, does not participate in the denoising process. The other U-net, namely DenoisingNet, is responsible for denoising process and generating videos guided by conditions provided by ReferenceNet and other modules.

As shown in Figure 2, the input of our method consists of three parts: 1) a single portrait image of an arbitrary identity, 2) a speech audio clip from an arbitrary person, and 3) optional user specified control signals. As for user control, our method support various forms of signals. For head motion control, users are allowed to use precise rotation angles around X, Y, and Z axes for each frame to generate desired head movement. Users can also provide a video or an image and extract its head pose with FLAME trackers as control signal. In addition, user can track and modify input video motions by changing its rotation angles to generate final movement. As a conclusion, FLAP only need a final angle in 6-DOF as control signal for pose, which allows users to freely overlay or modify head angles from different source to generate videos with desired head movements. Notably, if audio is provided, by overlaying mild head movements generated from audio with user-controlled movements, our method generates user-specified head actions while still preserving the subtle nodding when speaking, thus maintaining naturalness. If a fix head is needed, user can set head angle to a fixed value to generate talking head videos with fixed pose.

Intuitively, head movements and facial expressions are

closely tied with the tone and cadences in speech. To ensure such an interconnection, we bind head movements, facial expressions and lip movement to audio utilizing an audio-to-FLAME module. This module operate to generate natural head movement, expressions and lip movements from audio solely, avoided expression disruption from reference image. The detail of this module will be discussed in Section 4.4. And the visualization of this expression disruption in existing methods will be demonstrate in Section 5.7.

4.2. Controlling Diffusion Model with 3D Head Coefficient as Condition

In recent diffusion-based works like Follow-your-Emoji (Ma et al., 2024b), V-Express (Wang et al., 2024a) and EchoMimic (Chen et al., 2024), there has been a tendency to project landmark information into image space, and further serve as the condition to guide diffusion process. Although projected landmark images can be easily applied to control net like structures with out extra effort, it leads to a loss of head motions in 3D space. Additionally, 2D landmarks carry identity information which need careful design of alignment method across different input images. Problems are likely to arise when there is a large appearance variation in source image and driving video from which landmarks are extracted. Apart from the challenges in unifying landmarks to prevent id leakage, another problem of landmark-based approach is that there is hardly no landmark can be detected in stylized portraits, anime characters and portrait sculptures, making landmark alignment even more challenging.

To address above problems, we introduce 3D head coefficients which include head pose coefficients and facial expression coefficients to control diffusion model. In FLAP, our 3D head coefficients are based on FLAME, a parametric 3D head model. We use global rotation $\theta_{globalR} \in \mathbb{R}^3$ in Equation (2) as an additional diffusion condition for head control. $\theta_{globalR}$ is a sub-vector of θ , which denotes global head rotation in 6 DoF and is represented by 3 angles of rotation around x, y and z axis. For facial expression coefficients, we use $\theta_{jaw} \in \mathbb{R}^3$, $\theta_{eyes} \in \mathbb{R}^6$, $\psi_{eyelids} \in \mathbb{R}^2$ and $\psi_{exp} \in \mathbb{R}^{100}$ in Equation (2) for jaw movement, eye features, eyelids features and expressions. Thus, the proposed 3D head conditions for diffusion process in FLAP can be denotes as

$$c_{3Dhead} = [\theta_{globalR}, \theta_{eyes}, \theta_{jaw}, \psi_{eyelids}, \psi_{exp}] \quad (3)$$

Overall conditions for diffusion process can be summarize as $C = [C_{3Dhead}, c_{ref}]$, where C_{3Dhead} is a sequence of c_{3Dhead} that contains 3D head information varying over time, with each c_{3Dhead} corresponding to a frame in the video. We express this formally as $C_{3Dhead} = \{c_{3Dhead_1}, c_{3Dhead_2}, c_{3Dhead_3}, \dots, c_{3Dhead_n}\}$. For all coefficients mentioned above, we follow the settings of FLAME to open up opportunities to incorporate FLAP with other

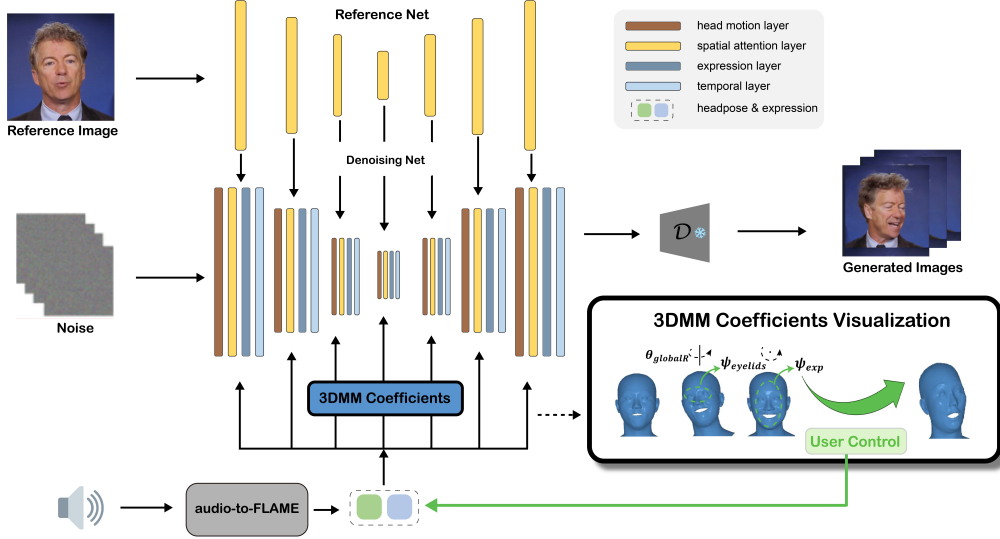


Figure 2. Model architecture of FLAP. The main diffusion net accept a generated 3D parameter input, which can also be modified and biased by user input. For audio only scenarios, FLAP utilizes an audio-to-FLAME module, which generate FLAME coefficients from audio. Our main U-net block consists of 4 layers, namely, head motion layer, spatial attention layer, expression layer and temporal layer. These layers are trained in different stages with different input conditions as we proposed Progressively Focused Training scheme, which will be discussed in Section 5.6.2

models in FLAME’s ecosystem such as EMOCA (Daněček et al., 2022), EMOTE (Daněček et al., 2023), and other works in upstream tasks.

The purpose of our DenoisingNet is to generate a video that both matches the 3D head information in C_{3Dhead} and the appearance information in c_{ref} . Thus, during training, we extract c_{3Dhead} for every frame in training video using FLAME fitting method (Zielonka et al., 2022). Then train the model to generate video frames given 3D head condition sequence C_{3Dhead} of target frames along with a reference image. Target video is used as supervision. The training objective can be formulated as follow:

$$L = \mathbb{E}_{z_t, c, \epsilon \sim \mathcal{N}(0,1), t} [\|\epsilon - \epsilon_\theta(z_t, t, C)\|_2^2] \quad (4)$$

where ϵ_θ denotes DenoisingNet. During inference, as shown in Figure 2, a given portrait image is feed into ReferenceNet to get c_{ref} . And a sequence of 3D head condition $\{c_{3Dhead_1}, c_{3Dhead_2}, c_{3Dhead_3}, \dots, c_{3Dhead_n}\}$ is generated by audio-to-FLAME module and then manipulated by user signals, and then feed into DenoisingNet to output a talking head video precisely controlled by 3D head conditions.

4.3. Progressively Focused Training for Expression-Motion Decoupling

Training process in previous methods (Tian et al., 2024; Ma et al., 2024b; Hu, 2024; Xu et al., 2024a; Wang et al., 2024a) is structured into two stages, namely image training stage and video training stage. For image training, two frames are randomly extracted from a video: one frame is used as the reference image, while the other serves as the target.

With reference image used as input for ReferenceNet, the whole model is trained to make predictions conditioned on given reference image without audio input. In video training stage, the model is trained to predict a continuous sequence of frames conditioned on both audio and reference image. However, 3D head coefficients delivers global pose information and detailed face information at the same time. Thus, when they are introduced as condition, model struggles to learn a correct patterns from massive volume of information within one stage.

Additionally, another significant challenge is learning a decoupled representation of facial expression and head pose. Although FLAME model itself decoupled facial expression from head pose, an unavoidable nature of monocular face 3D reconstruction is that the head has one side facing the camera while the other side is not. Thus, when using popular fitting methods (Zielonka et al., 2022; Retsinas et al., 2024) to reconstruct 3D head coefficients from monocular videos, it’s inevitable that head pose information will leak from expression coefficients. Given a video with only the left side of a talking face, 3D head fitting methods can not get correct coefficients of the other side of this face, leading to inaccuracies and flaws in the representation of the unseen half of face. Therefore, a pattern emerges that if certain facial coefficients appear anomalous, it indicates that this side of the head is not facing the camera. As a result, expression coefficients contain a learnable pattern of head pose information. This makes it easy to train a biased model. Visual results are provided in Section 5.6.2.

To address above issues, we proposed a Progressively Fo-

Table 1. Quantitative comparisons with existing works. 1 ★ in controllability means only support audio or video driven. 2 ★ indicates support both ways. 3 ★ means head pose and facial expression can be controlled independently. FLAP has 4 ★ since it not only supports all features above, but also supports angle input for nuance head pose manipulation and control. The best result for each metric is in **bold**, and the second-best result is underlined.

| Model | Controllability | Driven | FID↓ | FVD↓ | FaceIQ↑ | SYNC-C↑ | H-IQA↑ |
|--------------------|-----------------|--------|---------------|---------------|---------------|---------------|---------------|
| MCNet | ★ | video | - | - | 0.4001 | 7.4600 | 0.2992 |
| EchoMimic | ★ ★ | video | - | - | 0.5890 | 6.7896 | 0.3919 |
| EDTalk | ★ ★ ★ | video | - | - | 0.4159 | 8.4260 | 0.3018 |
| X-Portrait | ★ | video | - | - | 0.6544 | 5.8181 | 0.4795 |
| LivePortrait | ★ | video | - | - | 0.5474 | 7.6228 | 0.3987 |
| FLAP (ours) | ★ ★ ★ ★ | video | - | - | <u>0.6107</u> | <u>7.7837</u> | <u>0.4644</u> |
| SadTalker | ★ | audio | 163.31 | 551.94 | 0.4798 | 6.9274 | 0.3137 |
| EDTalk | ★ ★ ★ | audio | 166.11 | 592.20 | 0.4434 | 7.2472 | 0.3052 |
| EchoMimic | ★ ★ | audio | 148.91 | 500.56 | 0.6116 | 7.0341 | 0.4329 |
| AniPortrait | ★ | audio | <u>137.27</u> | 581.01 | 0.6518 | 7.6117 | 0.4920 |
| Hallo | ★ | audio | 139.54 | <u>457.43</u> | 0.610 | 7.5069 | 0.4417 |
| Hallo2 | ★ | audio | 141.54 | 483.95 | 0.5993 | <u>7.7184</u> | 0.4241 |
| FLAP (ours) | ★ ★ ★ ★ | audio | 136.54 | 399.78 | <u>0.6254</u> | 7.8617 | <u>0.4592</u> |

cused Training strategy (PFT) for training efficiency and expression-motion decoupling. Guided by a basic concept that models tend to learn global features of an image before focusing on the finer details. We divide 3D head conditions in FLAP into two groups: detailed expression conditions $c_{exp} = [\theta_{eyes}, \theta_{jaw}, \psi_{eyelids}, \psi_{exp}]$, and head motion condition $c_{motion} = [\theta_{globalR}]$. Head motion condition is learned in earlier stage, while expression conditions is learned in later stages. Thus, our progressively focused training strategy separate training process into three stages. The first stage is head motion stage, which we conduct image training with all layers trainable. In this stage, $c = [c_{head}, c_{ref}]$ is the only provided condition. The model is forced to focus on head pose changes between reference image and target image. The second stage is expression stage. In this stage, the model focus on learning facial expressions which includes eyes information θ_{eyes} and $\psi_{eyelids}$, jaw information θ_{jaw} and global expression information ψ_{exp} . The overall conditions in this stage can be formulated as $c = [c_{exp}, c_{ref}]$, where $c_{exp} = [\theta_{eyes}, \theta_{jaw}, \psi_{eyelids}, \psi_{exp}]$. To avoid coupling of expression and head motion, attention layers related to head motion are frozen. In the third stage, video training is conducted, we follow the settings in recent works (Tian et al., 2024; Xu et al., 2024a) to train Animatediff (Guo et al., 2023) blocks.

4.4. Audio to FLAME Module

Most existing diffusion methods trends to generate expressions and appearance jointly in a DenoisingNet with condition $c = [c_{audio}, c_{ref}]$. We argue that in training, the existence of c_{ref} can disrupt the learning of c_{audio} . From our observation, reference images carry more learnable informa-

tion of expressions than audio. Since the speaker’s emotion often show minimal variation in short videos. Therefore, the model will be misled to learn a biased pattern by simply copy the expressions of reference image to output video. For example, given a smiling face image and angry speech, model might generate a half-smiling video, fail to align with the angry audio input. More visual results of this observation can be found in Section 5.7.

To avoid c_{audio} being affected by c_{ref} , we utilize an audio-to-FLAME module which generate FLAME-based expression coefficients and head motion coefficients solely from audio. This helps us bind facial expressions and head motion to audio, eliminating c_{ref} ’s impact on expressions. Another advantage of this is that user can control pose and expression freely by manipulating FLAME coefficients. Benefiting from this architecture, users can also extract coefficients from other videos to accomplish video driven portrait animation tasks. An interactive model viewer¹ provided by the authors of FLAME visualize the mapping of FLAME parameters to the mesh output.

Generating head pose and expression from audio in 3DMM coefficients space is a well studied task (Sun et al., 2024; Peng et al., 2023). Our Audio-to-FLAME module follows the designed of (Wen et al., 2020). We retained the network with FLAME coefficients instead of BFM. As FLAME coefficients is portable, the audio-to-Flame module can be replaced by any FLAME coefficients generating methods such as EmoTalk(Peng et al., 2023),EMOTE (Daněček et al., 2023), DiffPoseTalk(Sun et al., 2024).

¹<https://flame.is.tue.mpg.de/interactivemodelviewer.html>



Figure 3. Qualitative comparisons. Our model achieves the most accurate pose control, visual quality and lip synchronization.



Figure 4. Visual Results on 3 dof head pose control and rich expressions. Expressions of reference images are all neutral

5. Experiments

5.1. Implement Details

Our model is trained on HDTF, Nersemble, Celebv-HQ, VFHQ, Celebv-text and data collected from youtube. All video frames are resized to 512×512 . For face reconstruction and tracking, we re-implemented MICA (Zielonka et al., 2022) for video tracking as our tracker to fit FLAME coefficients. The dimension of 3D head condition $\theta_{globalR}$, θ_{eyes} , θ_{jaw} , $\psi_{eyelids}$, and ψ_{exp} is 3, 12, 3, 2, and 100, respectively. In head motion training stage, we use videos with head motion coefficient variance in top 20% and train for 150,000 steps. For facial expression training and video training, we train our model with all data for 150,000 and 50000 steps.

5.2. Visual Results on Controllable Generation

Figure 4 presents some results generated by our method. Given a sequence of head angles as control signal, our model can generate film-like scene with an avatar performing user designed actions. The first row demonstrate two avatars

turning his/her head around and making a head-down gesture. The second row shows an avatar first looking around and then performing another sequence of user defined actions. In the third row, we demonstrate the model’s ability of generating life-like expressions for stylized characters and novel anime characters, despite our model being trained exclusively on real portrait videos. With these abilities, our model breaks down the barriers in filmmaking, enabling real contributions to the creative process.

5.3. Evaluation

5.3.1. QUANTITATIVE EVALUATION

As evidenced in our qualitative comparisons in Table 1, FLAP outperforms other methods on most of the metrics in audio driven task. We achieve the best FID, FVD, SYNC score and second best IQA. Among these baselines, our method offers the best controllability without compromising its audio driven functionality. For IQA scores, Aniportrait achieves the highest scores. However, we argue that Aniportrait tend to generate videos with less expression and

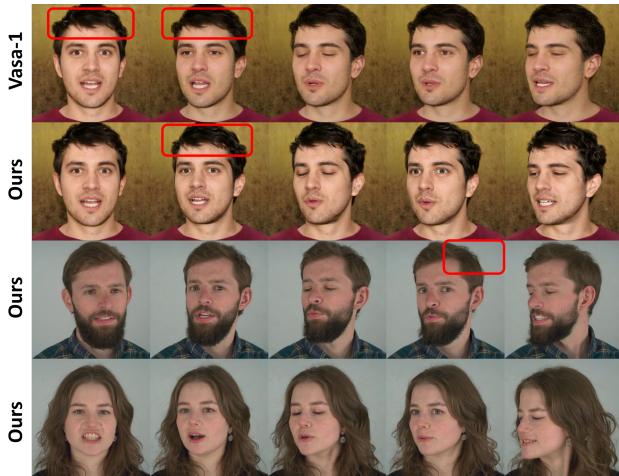


Figure 5. Comparison with VASA-1. The first column shows the reference image, the rest of the column shows generated results. The captions above shows the hair feature is gradually missing in VASA-1 demo video.

head movement so that there is less artifacts. We do a more detailed comparison with it in Section 5.5.

For video driven task, shown in Table 1, we do a cross-identity reenactment. Although EDtalk has the best Sync scores, its poor H-IQA and Face-IQA indicates its shortcoming in visual quality. X-portrait achieves the best visual quality, but has the worst lip synchronization among all methods. Our model achieve the second best in all metrics, successfully balanced visual quality and lip synchronization. It should be highlighted that our method only use a 120-dim FLAME coefficients vector for driving, while other methods rely on the entire video as their driving signal.

5.3.2. QUALITATIVE EVALUATION

For qualitative comparisons, as shown in Figure 3, our method generates the best results in common scenarios and scenarios with wide-range of head rotations, complex headpieces and makeup. Compared to our methods, Echomimic uses projected landmark images as control signal for generation and yields animations results with inaccurate pose and artifacts in headpieces. We perceive this inaccuracy as the loss of 3D pose information when projecting 3D key points to 2D images. As for X-portrait, it generate texture with high quality which results in better IQA scores, but it suffers from severe distortion around face and neck. Among all these methods, our method generate portrait videos with superior perceptual quality, motion precision and less artifact in both common scenarios and more complex scenarios.

5.4. Comparison with VASA-1

Since VASA-1 is not an open source project, we can only provide a qualitative comparison with its demo from the official website. As shown in Figure 5, the first column



Figure 6. Comparison with Landmark-based methods. The cropped images are only used for demonstration, we keep the all input dimensions as 512x512

demonstrates the original reference image, with his distinguishing hair feature highlighted in red box. We find that although VASA-1 achieve accurate pose control with user pre-defined angular information as ours method does, it suffers from the mean face problem as most GAN based decoders do. While the angle increase, the character starts losing its hair and face features and finally differs from original reference image. Vasa model seems tend to generate a face of an average man and fail to capture the detailed side profile feature of reference image. From our observation, this frequently happened in FaceVid2Vid(Wang et al., 2021) and Mega-Portrait. Vasa uses a retrained Mega-Portrait as its image encoder and decoder, which limits its expressiveness and causes this mean face problem. The third and the last rows shows that our method successfully avoid this mean face problem and generate detailed profile feature across different identities.

5.5. Comparison with Landmark-based methods

Prior studies like Aniportrait and Echomimic use facial landmarks as guidance for controllable generation. Here we provide a more detailed comparison between our method and Aniportrait. For Echomimic, visual comparison can be found in Figure 3. As shown in Figure 6, Lmk-based methods refers to Aniportrait. It is not capable of generating head movement like spinning and nodding since the projected 2D landmarks have lost most of the 3D pose information, thus offering vague pose information in denoising process. In Figure 6, the head generated by Aniportrait in the first 3 columns from left are all squished due to this projection error. In the remaining columns, aniportrait failed to generate accurate facial dynamics when there are significant differences between the driving identity and reference identity. As we discussed in former sections, these are the natural shortcomings of landmarks serving as control signals. However, in audio-driven mode, Aniportrait hardly generate head movement or dramatic facial expressions from audio, making it easier to maintain visual quality than other methods. On the other hand, our model use unified FLAME coefficients as conditions, avoiding the need for alignment and



Figure 7. Visual results of pose editing of a speech video. The first row shows the original video. We edit his head pose toward right in the second row.

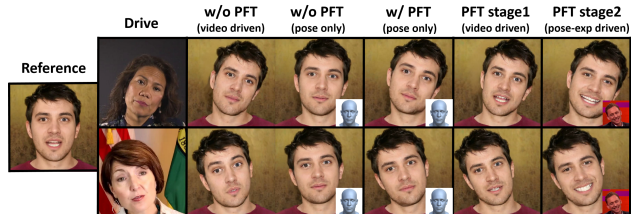


Figure 8. Ablation study on Progressive Focused Training (PFT). Pose only indicates that we use the expression coefficients from a canonical head who has a neutral face and canonical head pose (visualized at the bottom right of related images). By swapping original expression with this idle expression, we can explore whether the output head pose is affected by expression coefficients. And thus explore the head pose information leakage from expression coefficients. In the last column, the pose is driven by the 2nd column, while the expression is driven by the bottom right sub-image.

thus generating accurate facial dynamics and head pose as shown in Figure 6. Our approach demonstrates that FLAME coefficients can capture more subtle expressions, and is a more suitable as intermediate representation for controllable generation of talking head avatars.

5.6. Analysis and Ablation Study

5.6.1. ANALYSIS ON POSE EDITING

An example of our fine-grained control of expression and pose is demonstrated in Figure 1. Here we further demonstrate the visual results of pose editing of a speech video clip. In Figure 7, we edit the the orientation of the person’s head in the video clip without effecting his lip movement and expression (first row to second row). Our method exhibits the capability to disentangle pose and facial dynamics.

5.6.2. ABLATION STUDY

We conduct an ablation study to demonstrate the effectiveness of our proposed Progressively Focused Training (PFT) scheme. As is shown in the Figure 8 (the 2nd and 3rd left column), although FLAP can be trained to fit the source pose and expression well on video driven mode without PFT scheme, its head pose is heavily relied on signals leaked from expression coefficients, indicating failure in decoupling. To confirm this assumption, in the 4rd column, we set



Figure 9. Visual result of our method and Hallo2 (Cui et al., 2024) animating a smiling portrait with angry tone.

its expression coefficients idle, and get a result with decrease of head movement range. By contrast, in 5th column, when PFT is applied, the expression change will not affect head pose and achieve full disentanglement. In addition, when the model only completes the head motion training, it can only generate head motion aligning with pose source, but is not capable of modifying the expression of reference image (6th column). In the last column, when the model completes expression training stage, it’s capable of generating both head pose and expression from two different source. This decoupling of head pose and facial expression allows for independent control and shows the effectiveness of proposed PFT. Moreover, the proposed PFT scheme can be generalized to other conditions during training. We test this scheme using feature vectors from EDTalker (Tan et al., 2025) in supplementary.

5.7. Effectiveness of Audio-to-FLAME module

Our Audio-to-FLAME module is capable of binding the facial expression to audio, making all expressions irrelevant to reference image. As shown in Figure 9, Hallo2 struggles to generate appropriate expressions since it is confused by the smiling face in reference image and angry tone in the audio. Therefore, it generates a mixed and unnatural face. On the contrary, our model generate expressions solely relies on audio through our Audio-to-FLAME module, and thus generate accurate and natural expressions.

6. Conclusion

In this paper, we present FLAP, a novel approach for zero-shot talking-head avatar generation that integrates explicit 3DMM coefficients into a diffusion-based framework. By enabling independent control over head movements and facial expressions with PFT, FLAP significantly improves both naturalness and controllability of generated portrait videos. Our model demonstrates a nuanced understanding of 3D space, offering flexibility in controlling head movements and generating lifelike expressions from diverse sources. Extensive experiments show that FLAP outperforms existing methods in terms of visual quality lip synchronization and controllability, providing a promising solution for real-world applications.

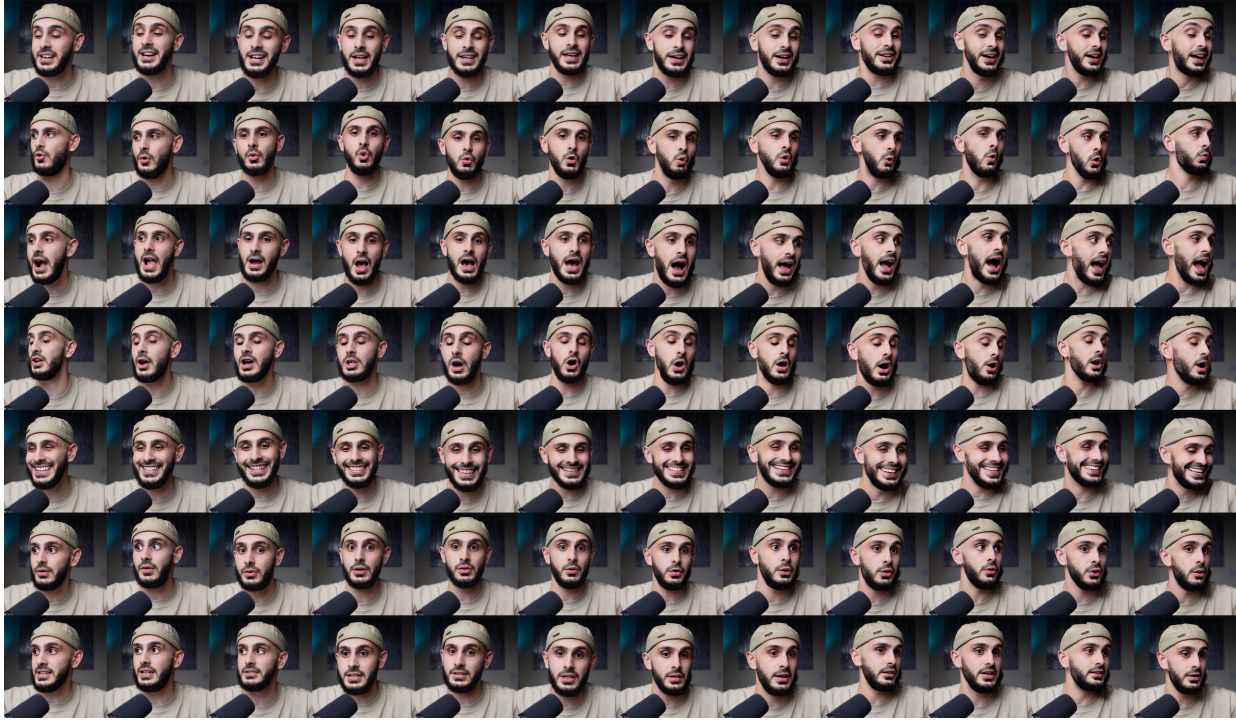


Figure 1. Additional Results on Multi-pose Generation

A. Appendix

A.1. Additional Results on Multi Pose Generation

Figure 1 provides more results of multi-pose and multi-expression generation of the same identity. The range of head rotation angle is pre-defined by a 3-dim vector representing $[x,y,z]$ angle in 3 DoF as control signal from user.

A.2. Flexibility Analysis

A.2.1. PORTABILITY OF FLAME COEFFICIENTS

As discussed in Sec4.4, FLAME coefficients is portable, making our audio-to-Flame module replaceable by any FLAME coefficients generating methods such as EmoTalk (Peng et al., 2023), EMOTE (Daněček et al., 2023), Diff-PoseTalk (Sun et al., 2024). For demonstration, we implemented a talking style controllable FLAME talker by integrating talking style control mechanism from (Zhang et al., 2023b) into Audio-DVP (Wen et al., 2020). Figure 2 demonstrates the visual results of integrating this style controlled Audio-DVP into FLAP. As shown in Figure 2, with this audio-dvp model, the style of mouth while speaking is changed, compared with original Audio-2-FLAME based FLAP, a greater degree of jaw opening is generated making it easier for lip reading. Thus, by combining with various existing methods, we can generate a range of speaking styles that we desire.

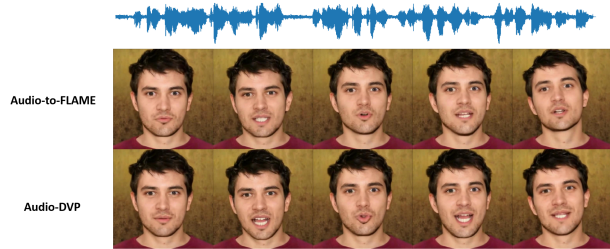


Figure 2. Visual result of integrating talking style from (Zhang et al., 2023b) into Audio-DVP(Wen et al., 2020) and cooperate with FLAP. The first row demonstrate original FLAP, while the second row shows the result of utilizing Audio-DVP + style control as a replacement of Audio-to-FLAME module.

A.2.2. USING FEATURE VECTORS AS CONDITIONS

FLAP exhibits a high level of flexibility as it can be integrated with existing models by using their feature vectors as diffusion condition. For example, EDtalk (Tan et al., 2025) and PD-FGC (Wang et al., 2023) proposed methods to extract implicit representations of facial expressions, head pose, lip pose and identity information from a single portrait image. Therefore, we can replace our 3D head head conditions in FLAP with feature vectors provided by EDtalk or PD-FGC. Figure 3 demonstrates the results of pose alignment using pose vector from PD-FGC. Figure 4 shows the results of independent control of pose and expression using pose and expression feature vector from EDTalk. Although



Figure 3. Visual results of FLAP framework cooperating with PD-FGC (Wang et al., 2023) by retraining FLAP using feature vectors from PD-FGC as conditions. We perform pose alignment of driving image using pose vector from PD-FGC.

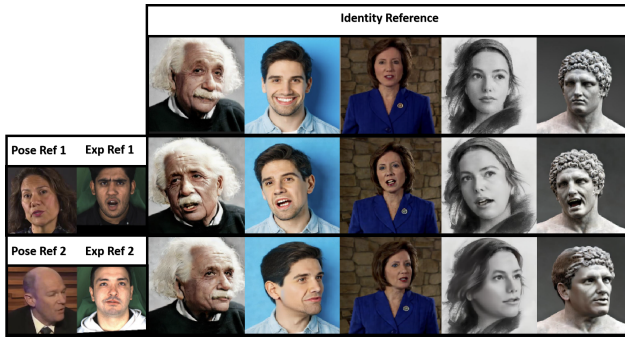


Figure 4. Visual results of FLAP framework cooperating with EDtalk (Tan et al., 2025). The first and second columns are head pose and expression references respectively. The first row shows the id reference. The others are generated results with mixed pose, expression and id of corresponding reference.

we achieve controllable using these feature vectors, its only yield results with less naturalness and expressiveness than our original model.

A.3. Additional Effectiveness Analysis of PFT Scheme

To test the generalize ability of our Progressively Focused Training (PFT) scheme, we retrained our FLAP frame work using feature vectors from EDtalk (Tan et al., 2025) as conditions for denoising. From our observation, the feature vector of EDtalk is not fully disentangled since its generator is trained to extract desired expression and pose information from these feature. Thus, PFT is necessary in training process to make sure disentanglement of pose and expressions. As shown in Figure 4, this retrained FLAP generates results with their pose aligned with pose reference image and expression aligned with expression reference image shown in the first two columns. This not only shows the generalize ability of PFT, but also demonstrate the flexibility of our model structure.

A.4. Hands Filtering in Data Pre-Processing

Filtering frames with hands in training data is crucial for the final generation results. As shown in Figure 5, existing open



Figure 5. Hand artifact of existing models.



Figure 6. Detection of a small part of the fingertip.

sourced models like Echomimic and Aniportrait is trained on unclean dataset in which hands often appears. To train a model that will not generate artifact of hands or fingers, we utilize Grounding Dino to detect hands and fingers every 3 frames in a video. As shown in Figure 6, even a little spot of finger can be detected and cut out from the video. Thus, we successfully trained a clean model on clean dataset.

A.5. More Animation Results

We provide more animation results in the next page, to demonstrate the generalization ability our our model and also to illustrate their visual quality. Please refer to Figure 7 in the **NEXT PAGE** to see diverse expressions, poses and styles of our generated results.

References

- Brooks, T., Holynski, A., and Efros, A. A. Instructpix2pix: Learning to follow image editing instructions. In *Proceedings of the IEEE/CVF Conference on Computer Vision and Pattern Recognition*, pp. 18392–18402, 2023.
- Burkov, E., Pasechnik, I., Grigorev, A., and Lempitsky, V. Neural head reenactment with latent pose descriptors. In *CVPR*, pp. 13786–13795, 2020.
- Cao, M., Wang, X., Qi, Z., Shan, Y., Qie, X., and Zheng, Y. Masactrl: Tuning-free mutual self-attention control for consistent image synthesis and editing. In *Proceedings of the IEEE/CVF International Conference on Computer Vision*, pp. 22560–22570, 2023.
- Chen, L., Maddox, R. K., Duan, Z., and Xu, C. Hierarchical cross-modal talking face generation with dynamic pixel-wise loss. In *Proceedings of the IEEE/CVF conference on computer vision and pattern recognition*, pp. 7832–7841, 2019.
- Chen, Z., Cao, J., Chen, Z., Li, Y., and Ma, C. Echomimic: Lifelike audio-driven portrait animations through editable landmark conditions. *arXiv preprint arXiv:2407.08136*, 2024.
- Cui, J., Li, H., Yao, Y., Zhu, H., Shang, H., Cheng, K., Zhou, H., Zhu, S., and Wang, J. Hallo2: Long-duration and high-resolution audio-driven portrait image animation. *arXiv preprint arXiv:2410.07718*, 2024.
- Daněček, R., Black, M. J., and Bolkart, T. Emoca: Emotion driven monocular face capture and animation. In *Proceedings of the IEEE/CVF Conference on Computer Vision and Pattern Recognition*, pp. 20311–20322, 2022.
- Daněček, R., Chhatre, K., Tripathi, S., Wen, Y., Black, M., and Bolkart, T. Emotional speech-driven animation with content-emotion disentanglement. In *SIGGRAPH Asia 2023 Conference Papers*, pp. 1–13, 2023.
- Drobyshev, N., Chelishev, J., Khakhulin, T., Ivakhnenko, A., Lempitsky, V., and Zakharov, E. Megaportraits: One-shot megapixel neural head avatars. In *Proceedings of the 30th ACM International Conference on Multimedia*, pp. 2663–2671, 2022.
- Fan, Y., Lin, Z., Saito, J., Wang, W., and Komura, T. Faceformer: Speech-driven 3d facial animation with transformers. In *Proceedings of the IEEE/CVF Conference on Computer Vision and Pattern Recognition*, pp. 18770–18780, 2022.
- Gong, Y., Zhang, Y., Cun, X., Yin, F., Fan, Y., Wang, X., Wu, B., and Yang, Y. Toontalker: Cross-domain face reenactment. In *Proceedings of the IEEE/CVF International Conference on Computer Vision*, pp. 7690–7700, 2023.
- Goodfellow, I., Pouget-Abadie, J., Mirza, M., Xu, B., Warde-Farley, D., Ozair, S., Courville, A., and Bengio, Y. Generative adversarial networks. *Communications of the ACM*, 63(11):139–144, 2020.
- Guo, J., Zhang, D., Liu, X., Zhong, Z., Zhang, Y., Wan, P., and Zhang, D. Liveportrait: Efficient portrait animation with stitching and retargeting control. *arXiv preprint arXiv:2407.03168*, 2024.
- Guo, Y., Yang, C., Rao, A., Liang, Z., Wang, Y., Qiao, Y., Agrawala, M., Lin, D., and Dai, B. Animatediff: Animate your personalized text-to-image diffusion models without specific tuning. *arXiv preprint arXiv:2307.04725*, 2023.
- He, Y., Yang, T., Zhang, Y., Shan, Y., and Chen, Q. Latent video diffusion models for high-fidelity long video generation. *arXiv preprint arXiv:2211.13221*, 2022.
- Ho, J., Jain, A., and Abbeel, P. Denoising diffusion probabilistic models. *Advances in neural information processing systems*, 33:6840–6851, 2020.
- Hu, E. J., Shen, Y., Wallis, P., Allen-Zhu, Z., Li, Y., Wang, S., Wang, L., and Chen, W. Lora: Low-rank adaptation of large language models. *arXiv preprint arXiv:2106.09685*, 2021.
- Hu, L. Animate anyone: Consistent and controllable image-to-video synthesis for character animation. In *Proceedings of the IEEE/CVF Conference on Computer Vision and Pattern Recognition*, pp. 8153–8163, 2024.
- Jiang, J., Liang, C., Yang, J., Lin, G., Zhong, T., and Zheng, Y. Loopy: Taming audio-driven portrait avatar with long-term motion dependency. *arXiv preprint arXiv:2409.02634*, 2024.
- Li, M., Yang, T., Kuang, H., Wu, J., Wang, Z., Xiao, X., and Chen, C. Controlnet: Improving conditional controls with efficient consistency feedback. In *European Conference on Computer Vision*, pp. 129–147. Springer, 2025.
- Li, R., Zhang, Y., Zhang, Y., Zhang, H., Guo, J., Zhang, Y., Liu, Y., and Li, X. Lodge: A coarse to fine diffusion network for long dance generation guided by the characteristic dance primitives. In *Proceedings of the IEEE/CVF Conference on Computer Vision and Pattern Recognition*, pp. 1524–1534, 2024.
- Li, T., Bolkart, T., Black, M. J., Li, H., and Romero, J. Learning a model of facial shape and expression from 4d scans. *ACM Trans. Graph.*, 36(6):194–1, 2017.

- Ma, Y., He, Y., Cun, X., Wang, X., Chen, S., Li, X., and Chen, Q. Follow your pose: Pose-guided text-to-video generation using pose-free videos. In *Proceedings of the AAAI Conference on Artificial Intelligence*, volume 38, pp. 4117–4125, 2024a.
- Ma, Y., Liu, H., Wang, H., Pan, H., He, Y., Yuan, J., Zeng, A., Cai, C., Shum, H.-Y., Liu, W., et al. Follow-your-emoji: Fine-controllable and expressive freestyle portrait animation. *arXiv preprint arXiv:2406.01900*, 2024b.
- Paysan, P., Knothe, R., Amberg, B., Romdhani, S., and Vetter, T. A 3d face model for pose and illumination invariant face recognition. In *2009 sixth IEEE international conference on advanced video and signal based surveillance*, pp. 296–301. Ieee, 2009.
- Peebles, W. and Xie, S. Scalable diffusion models with transformers. In *Proceedings of the IEEE/CVF International Conference on Computer Vision*, pp. 4195–4205, 2023.
- Peng, Z., Wu, H., Song, Z., Xu, H., Zhu, X., He, J., Liu, H., and Fan, Z. Emotalk: Speech-driven emotional disentanglement for 3d face animation. In *Proceedings of the IEEE/CVF International Conference on Computer Vision*, pp. 20687–20697, 2023.
- Qi, C., Cun, X., Zhang, Y., Lei, C., Wang, X., Shan, Y., and Chen, Q. Fatezero: Fusing attentions for zero-shot text-based video editing. In *Proceedings of the IEEE/CVF International Conference on Computer Vision*, pp. 15932–15942, 2023.
- Qian, S., Kirschstein, T., Schoneveld, L., Davoli, D., Giebenhain, S., and Nießner, M. Gaussianavatars: Photorealistic head avatars with rigged 3d gaussians. In *Proceedings of the IEEE/CVF Conference on Computer Vision and Pattern Recognition*, pp. 20299–20309, 2024.
- Retsinas, G., Filntisis, P. P., Danecek, R., Abrevaya, V. F., Roussos, A., Bolkart, T., and Maragos, P. 3d facial expressions through analysis-by-neural-synthesis. In *Proceedings of the IEEE/CVF Conference on Computer Vision and Pattern Recognition*, pp. 2490–2501, 2024.
- Rombach, R., Blattmann, A., Lorenz, D., Esser, P., and Ommer, B. High-resolution image synthesis with latent diffusion models. In *Proceedings of the IEEE/CVF conference on computer vision and pattern recognition*, pp. 10684–10695, 2022.
- Ruiz, N., Li, Y., Jampani, V., Pritch, Y., Rubinstein, M., and Aberman, K. Dreambooth: Fine tuning text-to-image diffusion models for subject-driven generation. In *Proceedings of the IEEE/CVF conference on computer vision and pattern recognition*, pp. 22500–22510, 2023.
- Shi, X., Huang, Z., Wang, F.-Y., Bian, W., Li, D., Zhang, Y., Zhang, M., Cheung, K. C., See, S., Qin, H., et al. Motion-i2v: Consistent and controllable image-to-video generation with explicit motion modeling. In *ACM SIG-GRAPH 2024 Conference Papers*, pp. 1–11, 2024.
- Siarohin, A., Lathuilière, S., Tulyakov, S., Ricci, E., and Sebe, N. First order motion model for image animation. *Advances in neural information processing systems*, 32, 2019.
- Song, J., Meng, C., and Ermon, S. Denoising diffusion implicit models. *arXiv preprint arXiv:2010.02502*, 2020.
- Sun, Z., Lv, T., Ye, S., Lin, M., Sheng, J., Wen, Y.-H., Yu, M., and Liu, Y.-j. Diffposetalk: Speech-driven stylistic 3d facial animation and head pose generation via diffusion models. *ACM Transactions on Graphics (TOG)*, 43(4): 1–9, 2024.
- Tan, S., Ji, B., Bi, M., and Pan, Y. Edtalk: Efficient disentanglement for emotional talking head synthesis. In *European Conference on Computer Vision*, pp. 398–416. Springer, 2025.
- Tian, L., Wang, Q., Zhang, B., and Bo, L. Emo: Emote portrait alive-generating expressive portrait videos with audio2video diffusion model under weak conditions. *arXiv preprint arXiv:2402.17485*, 2024.
- Wang, C., Tian, K., Zhang, J., Guan, Y., Luo, F., Shen, F., Jiang, Z., Gu, Q., Han, X., and Yang, W. V-express: Conditional dropout for progressive training of portrait video generation. *arXiv preprint arXiv:2406.02511*, 2024a.
- Wang, D., Deng, Y., Yin, Z., Shum, H.-Y., and Wang, B. Progressive disentangled representation learning for fine-grained controllable talking head synthesis. In *Proceedings of the IEEE/CVF Conference on Computer Vision and Pattern Recognition*, pp. 17979–17989, 2023.
- Wang, F.-Y., Huang, Z., Shi, X., Bian, W., Song, G., Liu, Y., and Li, H. Animatelcm: Accelerating the animation of personalized diffusion models and adapters with decoupled consistency learning. *arXiv preprint arXiv:2402.00769*, 2024b.
- Wang, T.-C., Mallya, A., and Liu, M.-Y. One-shot free-view neural talking-head synthesis for video conferencing. In *Proceedings of the IEEE/CVF conference on computer vision and pattern recognition*, pp. 10039–10049, 2021.
- Wang, Y., Guo, J., Bai, J., Yu, R., He, T., Tan, X., Sun, X., and Bian, J. Instructavatar: Text-guided emotion and motion control for avatar generation. *arXiv preprint arXiv:2405.15758*, 2024c.

- Wei, H., Yang, Z., and Wang, Z. Aniportrait: Audio-driven synthesis of photorealistic portrait animation. *arXiv preprint arXiv:2403.17694*, 2024.
- Wen, X., Wang, M., Richardt, C., Chen, Z.-Y., and Hu, S.-M. Photorealistic audio-driven video portraits. *IEEE Transactions on Visualization and Computer Graphics*, 26(12):3457–3466, 2020.
- Xie, Y., Xu, H., Song, G., Wang, C., Shi, Y., and Luo, L. X-portrait: Expressive portrait animation with hierarchical motion attention. In *ACM SIGGRAPH 2024 Conference Papers*, pp. 1–11, 2024.
- Xing, J., Xia, M., Zhang, Y., Cun, X., Wang, J., and Wong, T.-T. Codetalker: Speech-driven 3d facial animation with discrete motion prior. In *Proceedings of the IEEE/CVF Conference on Computer Vision and Pattern Recognition*, pp. 12780–12790, 2023.
- Xu, M., Li, H., Su, Q., Shang, H., Zhang, L., Liu, C., Wang, J., Yao, Y., and Zhu, S. Hallo: Hierarchical audio-driven visual synthesis for portrait image animation. *arXiv preprint arXiv:2406.08801*, 2024a.
- Xu, S., Chen, G., Guo, Y.-X., Yang, J., Li, C., Zang, Z., Zhang, Y., Tong, X., and Guo, B. Vasa-1: Lifelike audio-driven talking faces generated in real time. *arXiv preprint arXiv:2404.10667*, 2024b.
- Yang, S., Li, H., Wu, J., Jing, M., Li, L., Ji, R., Liang, J., Fan, H., and Wang, J. Megactor- σ : Unlocking flexible mixed-modal control in portrait animation with diffusion transformer, 2024. URL <https://arxiv.org/abs/2408.14975>.
- Ye, Z., Jiang, Z., Ren, Y., Liu, J., He, J., and Zhao, Z. Geneface: Generalized and high-fidelity audio-driven 3d talking face synthesis. *arXiv preprint arXiv:2301.13430*, 2023.
- Zhang, L., Rao, A., and Agrawala, M. Adding conditional control to text-to-image diffusion models. In *Proceedings of the IEEE/CVF International Conference on Computer Vision*, pp. 3836–3847, 2023a.
- Zhang, W., Cun, X., Wang, X., Zhang, Y., Shen, X., Guo, Y., Shan, Y., and Wang, F. Sadtalker: Learning realistic 3d motion coefficients for stylized audio-driven single image talking face animation. In *Proceedings of the IEEE/CVF Conference on Computer Vision and Pattern Recognition*, pp. 8652–8661, 2023b.
- Zhang, Y., Wei, Y., Jiang, D., Zhang, X., Zuo, W., and Tian, Q. Controlvideo: Training-free controllable text-to-video generation. *arXiv preprint arXiv:2305.13077*, 2023c.
- Zhou, H., Sun, Y., Wu, W., Loy, C. C., Wang, X., and Liu, Z. Pose-controllable talking face generation by implicitly modularized audio-visual representation. In *Proceedings of the IEEE Conference on Computer Vision and Pattern Recognition (CVPR)*, 2021.
- Zhou, Y., Han, X., Shechtman, E., Echevarria, J., Kalogerakis, E., and Li, D. Makeltalk: speaker-aware talking-head animation. *ACM Transactions On Graphics (TOG)*, 39(6):1–15, 2020.
- Zielonka, W., Bolkart, T., and Thies, J. Towards metrical reconstruction of human faces. In *European conference on computer vision*, pp. 250–269. Springer, 2022.